HHS Public Access

Author manuscript

Nat Methods. Author manuscript; available in PMC 2010 August 01.

Published in final edited form as:

Nat Methods. 2010 February ; 7(2): 126–129. doi:10.1038/nmeth.1412.

Chronic microsensors for longitudinal, subsecond dopamine detection in behaving animals

Jeremy J. Clark[1,4], **Stefan G. Sandberg**[1,4], **Matthew J. Wanat**[1], **Jerylin O. Gan**[1,2], **Eric A. Horne**[1], **Andrew S. Hart**[1,2], **Christina A. Akers**[1], **Jones G. Parker**[3], **Ingo Willuhn**[1], **Vicente Martinez**[1], **Scott B. Evans**[1], **Nephi Stella**[1,2], and **Paul E. M. Phillips**[1,2,*]

[1]Department of Psychiatry & Behavioral Sciences and Department of Pharmacology, University of Washington, Seattle, WA 98195, USA

[2]Graduate Program in Neurobiology & Behavior, University of Washington, Seattle, WA 98195, USA

[3]Department of Biochemistry, University of Washington, Seattle, WA 98195, USA

Abstract

Neurotransmission operates on a millisecond timescale, but is changed by normal experience or neuropathology over days, weeks or even months. Despite the great importance of long-term neurotransmitter dynamics, no technique exists to track these changes within a subject from day to day over extended periods of time. Here we describe and characterize a microsensor that can detect the neurotransmitter dopamine with subsecond temporal resolution over months *in vivo* in rats and mice.

The mesencephalic dopamine systems are a primary focus of research into motor control, motivation, and reinforcement learning1,2; and their disruption is implicated in many neurological and neuropsychiatric disorders, including Parkinson's disease, schizophrenia, substance abuse, and depression3,4. In particular, much attention focuses on the subsecond electrophysiological responses of dopamine neurons to behaviorally relevant stimuli including primary rewards, reward-predicting cues and novel objects1. Consequently, the detailed characterization of the activity of dopamine neurons and ensuing dopamine release

*Correspondence: pemp@uw.edu.

[4]These authors contributed equally to the work

Author contribution

P.E.M.P. conceived the work; S.B.E. optimized the microsensor design; J.J.C., S.G.S., N.S. and P.E.M.P. designed experiments and prepared the manuscript; J.J.C., S.G.S., M.J.W., J.O.G., E.A.H., A.S.H., J.G.P., C.A.A., I.W. and V.M. collected and analyzed data.

AOP

A chronically implanted biocompatible electrochemical microsensor allows long-term recording of subsecond dopamine dynamics *in vivo*. The microsensor can reliably detect behaviorally evoked dopamine release from dopamine neurons in the brain over a period of months in rats.

ISSUE

A chronically implanted biocompatible electrochemical microsensor allows long-term recording of subsecond dopamine dynamics *in vivo*. The microsensor can reliably detect behaviorally evoked dopamine release from dopamine neurons in the brain over a period of months in rats.

in target structures has been, and continues to be a highly active and important area of research.

Chemical approaches are necessary for the direct assessment of extracellular dopamine dynamics in target structures5. Classic neurochemical techniques, such as microdialysis, are ideal for measuring tonic baseline levels of neurotransmitters such as dopamine, but have low sampling rates (minutes) that cannot temporally resolve the rapid changes in extracellular dopamine concentration predicted by neurophysiological data. However, electrochemical techniques, such as fast-scan cyclic voltammetry (FSCV), can provide the necessary high-temporal-resolution detection. FSCV offers chemical selectivity to discriminate dopamine from other electroactive species in the brain by providing an electrochemical signature (cyclic voltammogram, CV) of the analyte. This methodology is used to detect subsecond changes in behaviorally evoked dopamine release after the presentation of salient stimuli and during behavioral tasks6–8. However, existing approaches are constrained by the requirement for acute implantation of a voltammetric probe into the brain via a microdrive for each experiment9, limiting the ability to track longitudinal changes in neurotransmitter dynamics over the course of disease progression in animal models, or throughout most learning paradigms10. Conversely, previous attempts to use chronically implanted electrodes to make long-term electrochemical measurements have met with limited success11–13. These studies conclude that the fidelity of chemical recordings can be severely impaired by perturbation of the microenvironment through physical tissue disruption and/or neuroinflammation, emphasizing that size and biocompatibility are critical considerations in the design of chronic devices for *in situ* neurochemistry14,15.

Here we describe a biocompatible voltammetric microsensor that can be chronically implanted into the targets of midbrain dopamine systems where it can detect subsecond dopamine dynamics from day to day over periods of months. This microsensor consists of a 7-μm diameter carbon fiber housed in a 90-μm diameter polyimide-covered fused-silica capillary (Fig. 1a). These microsensors produced a linear response to physiological concentrations of dopamine as assessed *in vitro* with flow injection analysis (Fig. 1b).

To determine the biocompatibility and suitability for long-term chemical recordings, we assessed the expression of glial markers and tyrosine hydroxylase (TH) using immunohistochemistry following chronic microsensor implantation. Striatal slices were prepared from rats implanted with microsensors for ten to sixteen weeks and stained for markers of microglia (Iba1) and astrocytes (glial fibrillary acidic protein; GFAP). Dopamine was detected *in vivo* at four of the five implantation sites tested. No glial encapsulation was found near the tract left by the 7-μm carbon fiber (Fig. 2a) in agreement with previous studies demonstrating that probes less than 12 μm in diameter are not encapsulated15. In some slices, we detected a small number of reactive astrocytes near the fused-silica shaft, as indicated by an increase in GFAP staining (Supplemental Fig. 1), and a small number of dispersed activated microglia, as evident by their condensed morphology. However, even around the tract left by the shaft, glial encapsulation was not evident. In comparison to control tissue, we found that TH immunostaining was decreased along the tract left by the fused silica shaft, but not at the site of the carbon fiber (Fig. 2a and Supplemental Fig. 1).

No differences in gliosis or TH staining were noted between the implantation sites of the four functional microsensors and that of the single microsensor that did not detect dopamine. Lack of dopamine detection in apparently healthy tissue is not surprising given previous findings demonstrating the heterogeneity in behaviorally evoked dopamine signals in the striatum16. Together, these results demonstrate that chronic implantation of the carbon fiber for up to four months does not result in overt reactive gliosis, encapsulation of the carbon fiber or a loss of TH expression, any of which could affect chemical detection.

To determine the stability of microsensor sensitivity during implantation, another set of rats (n = 14) were sacrificed approximately one, two or four months after implantation, and microsensor sensitivity to dopamine was tested in the flow-injection apparatus. The sensitivity of the microsensor was not significantly different between any of the implantation durations ($F_{(2,11)} = 0.012$, $P = 0.99$; Fig. 2b) and was similar to that for microsensors that had not previously been implanted (see Fig. 1b) indicating stability during chronic implantation for up to four months.

Next we tested the ability of the chronically implanted microsensor to detect dopamine *in vivo*. The functionality of a voltammetry electrode can be assessed by measuring fluctuations in dopamine release after electrical stimulation of the ventral tegmental area (VTA), substantia nigra pars compacta (SNc), or the medial forebrain bundle6. Using the chronically implanted microsensor, electrically evoked dopamine release in the nucleus accumbens (NAc) was detected and was comparable with that obtained with acute voltammetry electrodes here (Fig. 2c) and in previous reports6. FSCV is known to confer temporal distortion to *in vivo* dopamine signals17. However, we noted that there was more temporal distortion in the response from the chronically implanted microsensor compared to an acutely implanted electrode (Supplementary Fig. 2). While this process does not impair the detection of changes in phasic signaling amplitude during learning or in disease models, mathematical deconvolution procedures may be useful for precise kinetic analysis17.

Electrically evoked neurochemical signals provide a reliable means to assess the functionality of specific recording electrodes but behaviorally evoked signals, such as reward presentation, are often more experimentally relevant. Delivery of natural rewards has been shown to increase the firing of dopamine neurons in the VTA and SNc in monkeys1 and elicits dopamine release in the NAc in rats7. The chronic microsensor is also effective at detecting dopamine release to this type of stimulus (Fig. 2c). The CV corresponding to the food-evoked signal is significantly correlated with an electrically evoked signal from the same microsensor (Fig. 2c; $r^2 \geq 0.75$), indicating that the behaviorally evoked signal is reliably identified as dopamine by established signal identification methods (CV analysis). In addition, a comparison of CVs obtained *in vitro* and under a variety of conditions *in vivo* revealed a significant correlation for all observations ($r^2 \geq 0.75$; Supplementary Fig. 3). Importantly, this relationship was similar to that for acute electrode preparations (Supplementary Fig. 3). The behaviorally evoked signal was further validated by demonstrating that it could be attenuated by inactivation of the VTA, the primary dopamine innervation to the NAc (Supplementary Fig. 4). Collectively this electrochemical and pharmacological characterization together with the anatomical, physiological and

independent verification presented in the Supplementary Note provides a high degree of confidence that the recorded signal is dopamine.

To assess the longevity of dopamine detection with this approach, twenty microsensors were chronically implanted and repeatedly tested for their ability to detect behaviorally evoked dopamine release, verified by CV analysis (Fig. 3a). There are several potential sources of electrode attrition relevant to maintaining chronic recordings; therefore all electrodes were included in the analysis regardless of their failure mode (Supplementary Table 1). Four microsensors failed prior to dopamine detection. The remaining sixteen microsensors were capable of detecting dopamine for a period ranging from one and a half to four months post surgery.

Behaviorally evoked dopamine release in the NAc was reliably detected at one, two and four months post implantation (Fig. 3b). CVs obtained from reward-evoked dopamine release at these time points and those obtained from electrically evoked release at one and two months post surgery were significantly correlated with each other and those obtained *in vitro* (Supplementary Table 2). This maintained fidelity *in vivo* is consistent with the demonstration that microsensor sensitivity is stable over months after implantation. Finally, we monitored electrochemical signals during multiple-day reinforcement learning to demonstrate the potential of combining a chronically implantable microsensor with FSCV in assessing the dynamics of phasic dopamine release events over time. A specific role for dopamine in reinforcement learning is suggested by data from numerous paradigms2. Indeed, previous work with FSCV has demonstrated phasic dopamine release events in response to primary rewards and their predictors8. However, a complete characterization of phasic dopamine events in response to conditioned and unconditioned stimuli throughout learning has remained elusive due to methodological constraints10, which can be overcome by the current approach. The surface plots depict fluctuations in dopamine concentration recorded in the NAc by the chronic microsensor during every trial across twenty five days of training on a pavlovian conditioned approach task in a representative animal (Fig. 3c). These data clearly illustrate the trial-by-trial shift in phasic dopamine responses from reward presentation to a predictive cue during acquisition (days 1–5) and a persistent cue response during extended training (days 6–10). The capacity to sample from the same subject throughout all behavioral manipulations reveals the modulation of reward-evoked responses by changes in reward value (increased reward days 16–20) and the attenuation of cue-evoked responses during extinction (reward omission days 21–25).

The advantage of our approach lies in the ability to obtain multiple, repeated recordings in a single subject over a period of days, weeks or months. In addition to the assessment of the neurochemical correlates of psychological processes such as learning and memory, research aimed at exploring dopamine in animal models of psychiatric or neurological disorders will benefit from the capacity to measure during all aspects of the modeled disorder18,19. While the longitudinal data presented here were collected in rats, this microsensor has successfully been used for long-term, *in vivo* neurochemical measurements in mice (Supplementary Fig. 3). The now widely used manipulation of the mouse genome makes this an attractive species for the study of disease processes. Finally, this approach also permits the simultaneous assessment of dopamine release in multiple brain nuclei within a single subject

(Supplementary Fig. 5), a manipulation not possible with currently available methodology. These additional applications have the potential to extend the already rich field of *in vivo* voltammetry and allow researchers to make new inquiries and approach long-standing questions in a novel way.

Methods

Microsensor fabrication

Dopamine microsensors for chronic implantation consisted of carbon-fiber microelectrodes insulated in a fused-silica capillary20,21. A single carbon fiber (34–700, Goodfellow Corporation, PA) was inserted into a 10–15 mm length of fused silica (Polymicro Technologies, AZ) while submerged in 2-propanol. One end of the microsensor was then sealed with Devcon two-component epoxy (IWT Performance Polymers, FL) and allowed to dry, leaving a length of carbon fiber protruding. A silver connector (Newark, IL) was secured in contact with the carbon fiber on the other end of the silica with silver epoxy (8331; MG Chemicals, BC, Canada), allowed to cure overnight, then insulated with a layer of two component epoxy. After an additional twelve hours of drying, the fabrication of the chronic microsensor was finalized by trimming the exposed carbon fiber to the desired length of the sensor (150–200 μm).

Electrochemical Instrumentation

During voltammetric analysis, analyte electrolysis is driven by applying an electrical potential via an electrode, and chemical information is provided in the ensuing current, measured at the electrode. For all recordings, the applied potential to the microsensor was held at −0.4 V vs Ag/AgCl between voltammetric scans, and then ramped to +1.3 V and back at 400 V/s during the scan (8.5 ms total scan time). Voltammetric scans were repeated every 100 ms to obtain a sampling rate of 10 Hz. When dopamine is present at the surface of the electrode during a voltammetric scan, it is oxidized during the anodic sweep to form dopamine-*o*-quinone (peak reaction at approximately +0.7 V) which is reduced back to dopamine in the cathodic sweep (peak reaction at approximately −0.3 V). The ensuing flux of electrons is measured as current and is directly proportional to the number of molecules that undergo the electrolysis. For the chemical identification of dopamine, current during a voltammetric scan can be plotted against the applied potential to yield a CV. The CV provides a chemical signature that is characteristic of the analyte, allowing resolution of dopamine from other substances. For quantification of changes in dopamine concentration over time, the current at its peak oxidation potential can be plotted for successive voltammetric scans. Waveform generation, data acquisition and analysis were carried out on a PC-based system using uses two PCI multifunction data acquisition cards and software written in LabVIEW (National Instruments, TX). Signals were transmitted from chronically implanted microsensors to the data acquisition system via a head-mounted voltammetric amplifier (current-to-voltage converter) and an electrical swivel (Crist Instrument Co., MD) mounted above the recording chamber. The voltammetric amplifier consisted of an operational amplifier with a feedback resistor (R_f; 5 MΩ) which determined the current-to-voltage ‘gain’ (following Ohm’s Law: $V_{out} = I_{in} \times R_f$). In addition, a capacitor (6 pF) was connected in parallel with the feedback resistor to filter high frequencies, while other

capacitors bridged each of the power sources (+15 V, −15 V) with ground to filter operational amplifier noise. As reported elsewhere22, there is commonly a 200 mV shift in the reference potential at implanted Ag/AgCl electrodes. This change can be diagnosed by the position of Faradaic peaks within the background current and, when observed, the applied potential was offset by 200 mV to compensate, as previously described23.

Assessment of Electrode Sensitivity

The sensitivity of the microsensor to dopamine was determined *in vitro* before and/or after one, two, and four months implantation in brain using flow injection analysis. Briefly, the microsensor was placed in a flowing stream of artificial cerebrospinal fluid (ACSF; 3 ml/min) and electrochemical measurements were made with FSCV using the same parameters used for *in vivo* recordings. A time-dependent square pulse of dopamine (dissolved in ACSF) was introduced into the flow stream via an injection valve (V-1451-DC; Upchurch Scientific, WA). The sensitivity of the microsensor was determined by dividing the change in the voltammetric signal during introduction of dopamine by its concentration.

Voltammetry Surgery

All animal procedures presented in this paper followed the University of Washington Institutional Animal Care and Use Committee guidelines. Surgical preparation for *in vivo* voltammetry used aseptic technique. Male rats weighing between 300g and 350g (Charles River, CA) were anesthetized with isoflurane and placed in a stereotaxic frame. The scalp was swabbed with 10% povidone iodine, bathed with a mixture of lidocaine (0.5 mg/kg) and bupivicaine (0.5 mg/kg), and incised to expose the cranium. Holes were drilled and cleared of dura mater above the nucleus accumbens core (1.3-mm lateral and 1.3-mm rostral from bregma), the dorsolateral striatum (4.3-mm lateral and 1.2-mm rostral from bregma), and/or the nucleus accumbens shell (0.8-mm lateral and 1.2-mm rostral from bregma) for microsensors, above the midbrain (1.0-mm lateral and 5.2-mm caudal from bregma) for a stimulating electrode in some animals, and at convenient locations for a reference electrode and three anchor screws. The reference electrode and anchor screws were positioned and secured with cranioplastic cement, leaving the stimulating electrode and working electrode holes exposed. The microsensors were then attached to the voltammetric amplifier and lowered into the target recording regions (7.0-mm ventral of dura mater for nucleus accumbens, 4.0-mm ventral of dura mater for dorsolateral striatum). For animals in which a stimulating electrode was implanted, the voltammetric waveform was applied at 10 Hz and dopamine monitored. Next, the stimulating electrode (Plastics One, VA) was lowered 7.0 mm below dura mater and electrical stimulation (60 biphasic pulses, 60 Hz, ±120 μA, 2 ms/phase) was applied via an optically isolated, constant-current stimulator (A-M Systems, WA). If an evoked change in dopamine concentration was not observed at the working electrode, the stimulating electrode was positioned 0.2 mm more ventral. This was repeated until dopamine efflux was detected following stimulation. It was then lowered further in 0.1-mm increments until dopamine release was maximal. This is usually when the stimulating electrode is 8.4-mm ventral from dura mater. Finally, cranioplastic cement was applied to the part of the cranium that is still exposed to secure the stimulating electrode and microsensor(s).

Recording Sessions

In vivo experiments were carried out in a standard operant chamber (Med Associates, VT). A subset of animals was trained on a conditioned pavlovian approach (autoshaping) task. Each trial in an autoshaping session consisted of an eight-second presentation of a lever/light cue (conditioned stimulus) followed immediately by the delivery of a food pellet (unconditioned stimulus). Each training session (one per day) was comprised of 25 trials presented on a 60-second variable-interval schedule. After 15 sessions of standard training the reward value was increased from one to four food pellets for five days followed by five days of extinction training where food reward was omitted.

Pharmacological Validation

Animals were implanted with chronic, carbon fiber microsensors targeted at the nucleus accumbens core (1.3-mm lateral and 1.3-mm rostral from bregma) and with bilateral guide cannulae (26 gauge; Plastics One, VA) directed at the VTA (0.5-mm lateral and −5.6-mm caudal to bregma, lowered 7.0 mm ventral from dura mater). Dummy canulae (Plastics One, VA) were installed in the guide cannulae and removed during testing. On test days (~2 months after implantation), injectors (33 gauge; Plastics One, VA) were inserted through the guide cannulae so they protruded 1 mm beyond the guide cannulae to a final depth of 8.0 mm ventral from dura mater. Injections (0.5 μl) of ACSF (in mM: 154.7 Na^+, 2.9 K^+, 132.49 Cl^-, 1.1 Ca^{2+} at pH = 7.4) or baclofen (50 ng) dissolved in ACSF were visually monitored for accuracy and were completed within four min. Dopamine responses to reward delivery were recorded immediately prior to injections and 5 min after injections. Voltammetric responses were analyzed by calculating the area under the curve of the change in current at the peak dopamine oxidation potential which was normalized to the percentage of that for the pre-injection reward delivery.

Quad Multi-Site Recording Under Anesthesia

For proof of principle of recording at more than two electrodes, quad multi-site recordings were carried out at acutely implanted microsensors (identical construction to the chronic microsensor) in anesthetized animals during terminal surgery. Rats were anesthetized with urethane (1.5 g/kg, i.p.) and immobilized in stereotaxic frame. Body temperature was maintained with a deltaphase heating pad (Braintree scientific, MA). A midsagittal incision was placed slightly anterior and posterior of bregma and lambda, respectively. Connective tissue was removed to allow holes to be drilled (1.3-mm anterior, and 1.3-, 2.3-, 3.3- and 4.3-mm lateral of bregma). Upon careful removal of dura mater microsensors were lowered to 7.0-, 6.0-, 5.0- and 4.0-mm ventral of the pial surface. In addition a hole for stimulating electrode placement was made 4.6-mm posterior to and 1.3-mm lateral of bregma. For optimal dopamine release, the stimulating electrode was lowered at 0.1 mm increments starting at 7.0 mm until release was observed at all four microsensors. Electrically evoked dopamine was elicited by a 60-Hz, 120-pulse train with 4-ms wide bi-phasic square pulses at 300 μA (optically isolated and constant current). After completion of experiment, positions of microsensors were histologically verified.

Histological verification of recording sites

On completion of experimentation, animals were deeply anesthetized with intraperitoneal ketamine (100 mg/kg) and xylazine (20 mg/kg) and were then transcardially perfused with saline. The skull was carefully removed so that the attached microsensor remained intact. The brain was then removed and post-fixed in paraformaldehyde for twenty four hours and then rapidly frozen in an isopentane bath (~5 min). The brain was then blocked, sliced on a cryostat (50-μm coronal sections, 20 °C) and placed on slides. Slices were stained with cresyl violet to aid visualization of anatomical structures and the microsensor was localized by following the tract made by the fused-silica shaft. In a subset of animals, an electrolytic lesion (300 V) was made by applying current directly through the recording microsensor for 20 s to expedite histological identification of the recording site. However, lesioning typically alters the microsensor surface prohibiting accurate post-implantation assessment of *in vivo* sensitivity.

Data Analysis

Electrochemical data was analyzed using software written in LabVIEW (National Instruments, TX). All statistical analyses were carried out using Prism (GraphPad Software, CA). For every recording session, the chemical signature of behaviorally evoked phasic dopamine release was statistically compared to an *in vivo* template of dopamine. These templates were obtained from electrically evoked dopamine release after stimulation of the VTA or medial forebrain bundle taken from an early recording session. Behaviorally evoked signals met electrochemical criterion for dopamine if the cyclic voltammogram was closely correlated with that of stimulated release ($r^2 \geq 0.75$)24.

Immunohistochemistry

Seven male, Sprague-Dawley rats each with a microsensor that had been implanted 10–16 weeks earlier were perfused-fixed with 4-% paraformaldhyde. Their brains were cryoprotected (15-% sucrose for 24 hours followed by 30-% sucrose until they sank) and were stored at −80°C. Serial coronal sections (30 μm) were cut on a cryostat and stored in phosphate-buffered saline (PBS; 4 °C for up to 24 hours). For each animal, at least three consecutive sections were selected in which the electrode tract was visually identified close to the target structure. Two additional coronal slices rostral to the electrode tract were selected for secondary-only control and image analysis (see below). Slices were washed in PBS (3 times at room temperature, RT), blocked and permeablized with PBS supplemented with both donkey serum (5%) and Triton X-100 (1%) (under gentle agitation, 90 min at RT). Slices were then incubated under gentle agitation for 18–24 hrs at 4°C with primary antibodies prepared in PBS supplemented with donkey serum (2.5%) and Triton X-100 (0.5%) at the appropriate final concentrations as follows: Iba-1 (rabbit IgG, 1:400, Wako), α-GFAP (chicken IgY, 1:600, Millipore), α-tyrosine hydroxylase (mouse IgG, 1:1000, Millipore), donkey α-rabbit Alexa-488 (1:500, Invitrogen), donkey α-chicken Texas Red (1:125, Fitzgerald Industries International, Inc.) and donkey α-mouse Alexa-647 (1:500, Invitrogen). For each animal, one control slice did not receive any primary antibody (for secondary-only control). Slices were then washed six times with PBS supplemented with Tween-20 (0.05%) (10 min each at RT), and incubated with the appropriate secondary

antibodies prepared in PBS supplemented with donkey serum (2.5%) and Triton X-100 (0.5%) (1 hr at RT). Slices were then washed six times with PBS supplemented with Tween-20 (0.05%) (under gentle agitation at RT, 10 min each), followed by a brief wash in distilled water. All slices from the same animal were mounted onto a charged slide (Fisher brand Superfrost/Plus, Fisher Scientific) and allowed to dry for 18–24 hours. Cover slips were mounted with Vectashield (Vector Labs) and sealed with nail polish.

Microscopy and Image Analysis

Fluorescent images were collected using a Zeiss Axio Observer Z1 equipped with a Pan-Apochromatic 10x/0.3 PH1 DICI (Z-stack images at 3.42 μm) using Axiovision software. Identical exposure settings were used for the experimental, non-tract control and secondary-only controls. Intensities for TH were measured at two levels in Axiovision: 100-μm below end of the fused-silica tract (at the level of the carbon fiber) and 500-μm above the end of the fused-silica tract. This was carried out by drawing a band, 10-pixels wide and 300-μm long, on a six Z-stack compressed image. For data presentation, compressed Z-stack images were created in Axiovision and saved as Tiff files. The composite images were gated to background using the secondary-only control and the composites were aligned by hand in Photoshop (Adobe). Analysis of TH intensity at the level of the fused silica, the carbon fiber, and in control tissue was carried out by calculating z-scores for each sample based on the mean and standard deviation of control tissue.

Supplementary Material

Refer to Web version on PubMed Central for supplementary material.

Acknowledgements

We thank S. Barnes for technical assistance, and M. Walton and W. Shain for useful discussion. This work was supported by the University of Washington Royalties Research Fund and the National Institutes of Health (R01-MH079292, P.E.M.P; R21-DA024140, P.E.M.P; R01-DA014486, N.S.). J.J.C. was supported by F32-DA024540 (J.J.C.), M.J.W. was supported by T32-AA007455 (Larimer), J.O.G. was supported by T32-GM007270 (Kimelman), and A.S.H., J.G.P. and E.A.H. were supported by T32-DA007278 (Chavkin).

References

1. Schultz W, Dayan P, Montague PR. Science. 1997; 275:1593–1599. [PubMed: 9054347]
2. Wise RA. Neuron. 2004; 36:229–240. [PubMed: 12383779]
3. Hornykiewicz O, Kish SJ. Adv. Neurol. 1987; 45:19–34. [PubMed: 2881444]
4. Nestler EJ, Carlezon WA. Biol. Psychiatry. 2006; 59:1151–1159. [PubMed: 16566899]
5. Montague PR, McClure SM, Baldwin PR, Phillips PEM, Budygin EA, Stuber GD, Kilpatrick MR, Wightman RM. J. Neurosci. 2004; 24:1754–1759. [PubMed: 14973252]
6. Phillips PEM, Stuber GD, Heien ML, Wightman RM, Carelli RM. Nature. 2003; 422:614–618. [PubMed: 12687000]
7. Roitman MF, Stuber GD, Phillips PEM, Wightman RM, Carelli RM. J. Neurosci. 2004; 24:1265–1271. [PubMed: 14960596]
8. Day JJ, Roitman MF, Wightman RM, Carelli RM. Nat. Neurosci. 2007; 10:1020–1028. [PubMed: 17603481]
9. Phillips, PEM.; Robinson, DL.; Stuber, GD.; Carelli, RM.; Wightman, RM. Drugs of Abuse: Neurological Reviews and Protocols. Wang, JQ., editor. Totowa, NJ: Humana Press; 2003. p. 443-464.

10. Owesson-White CA, Cheer JF, Beyene M, Carelli RM, Wightman RM. Proc. Natl. Acad. Sci. U. S. A. 2008; 105:11957–11962. [PubMed: 18689678]
11. Kruk ZL, Cheeta S, Milla J, Muscat R, Williams JE, Willner P. J. Neurosci. Methods. 1998; 79:9–19. [PubMed: 9531455]
12. Duff A, O'Neill RD. J. Neurochem. 1994; 62:1496–1502. [PubMed: 7510782]
13. Wilson GS, Johnson MA. Chem. Rev. 2008; 108:2462–2481. [PubMed: 18558752]
14. Szarowski DH, Andersen MD, Retterer S, Spence AJ, Isaacson M, Craighead HG, Turner JN, Shain W. Brain Res. 2003; 983:23–35. [PubMed: 12914963]
15. Seymour JP, Kipke DR. Biomaterials. 2007; 28:3594–3607. [PubMed: 17517431]
16. Wightman RM, Heien MLAV, Wassum KM, Sombers LA, Aragona BJ, Khan AS, Ariansen JL, Cheer JF, Phillips PEM, Carelli RM. Eur. J. Neurosci. 2007; 26:2046–2054. [PubMed: 17868375]
17. Venton BJ, Troyer KP, Wightman RM. Anal. Chem. 2002; 74:539–546. [PubMed: 11838672]
18. Martin SJ, Grimwood PD, Morris RG. Annu. Rev. Neurosci. 2000; 23:649–711. [PubMed: 10845078]
19. Tolias AS, Ecker AS, Siapas AG, Hoenselaar A, Keliris GA, Logothetis NK. J. Neurophysiol. 2007; 98:3780–3790. [PubMed: 17942615]
20. Swiergiel AH, Palamarchouk VS, Dunn AJ. J. Neurosci. Methods. 1997; 73:29–33. [PubMed: 9130675]
21. Gerhardt GA, Ksir C, Pivik C, Dickinson SD, Sabeti J, Zahniser NR. J. Neurosci. Methods. 1999; 87:67–76. [PubMed: 10065995]
22. Moussy F, Harrison DJ. Anal Chem. 1994; 66:674–679. [PubMed: 8154589]
23. Heien ML, Khan AS, Ariansen JL, Cheer JF, Phillips PEM, Wassum KM, Wightman RM. Proc. Natl. Acad. Sci. U. S. A. 2005; 102:10023–10028. [PubMed: 16006505]
24. Cheer JF, Wassum KM, Heien MLAV, Phillips PEM, Wightman RM. J. Neurosci. 2004; 24:4393–4400. [PubMed: 15128853]

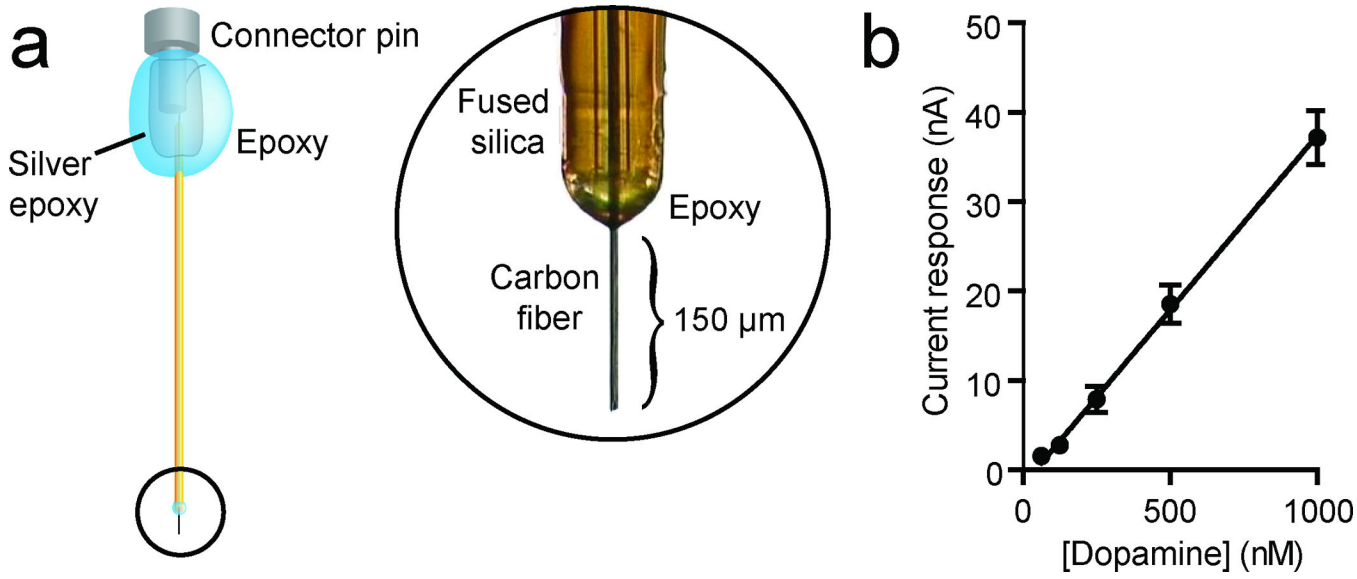

Figure 1. Chronic carbon-fiber microsensor

(a) All chronic microsensors used in these experiments consisted of a carbon fiber encased in a polyimide fused silica. In order to ensure electric insulation, a two-component epoxy was applied to the fused silica carbon fiber interface. At the opposite end, a female pin connector was electrically connected to the carbon fiber with silver epoxy. Finally, two-component epoxy was used to coat the connector for electrical insulation and structural integrity. **(b)** The response of the microsensor was found to be linear to physiological concentrations of dopamine ($n = 5$, $r^2 = 0.92$, $P < 0.0001$). Data are mean ± s.e.m.

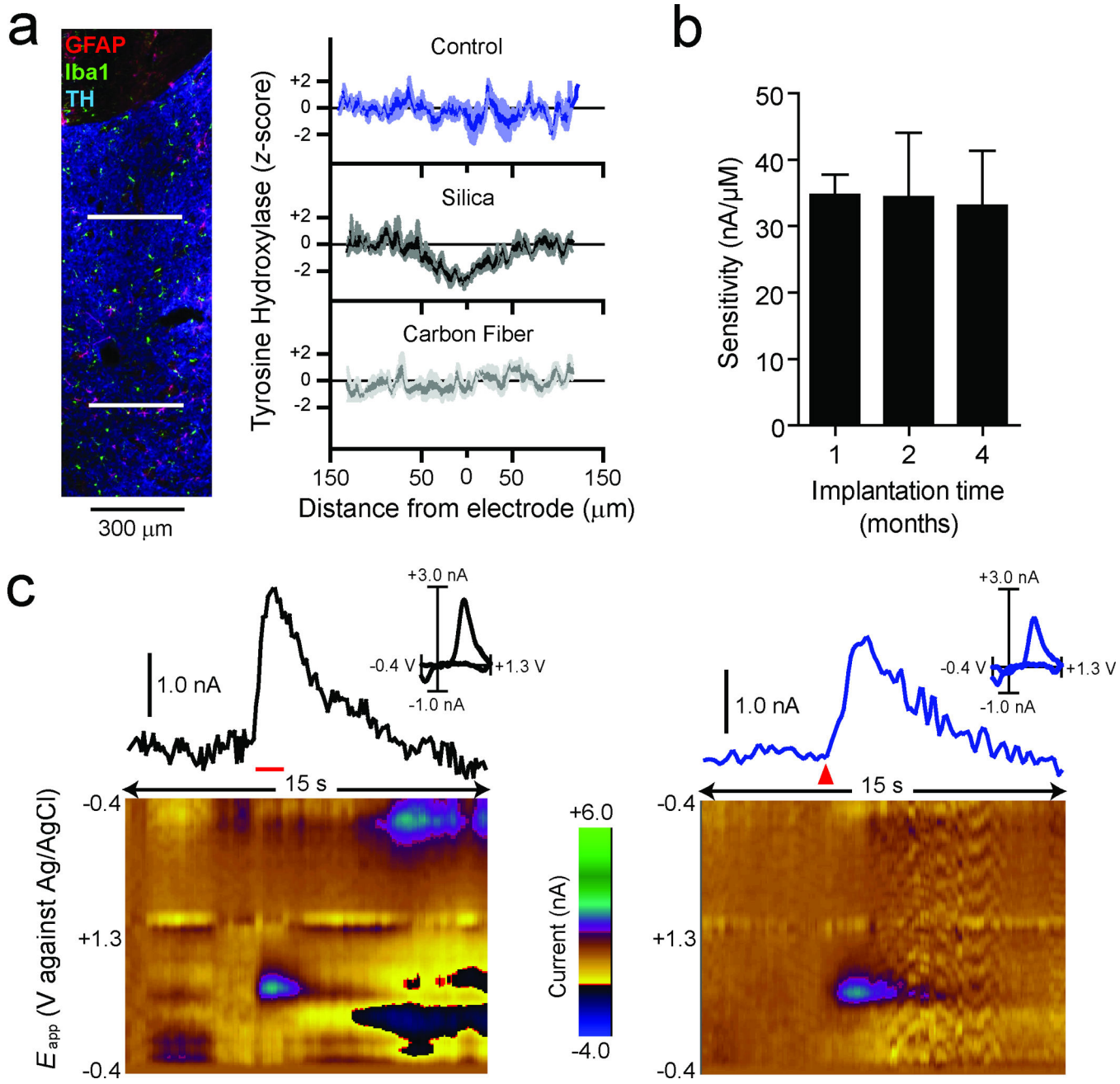

Figure 2. ***In vivo*** **fidelity of chronic carbon-fiber microsensors**

(a) 30-μm striatal slices were stained for astrocytes (GFAP, red), microglia (Iba1, green), and tyrosine hydroxylase (TH, blue). The composite image (left) shows the microsensor tract ending ventral to the anterior commissure with no apparent gliosis present. Line scans of TH intensities (right) were made across the fused-silica tract (upper white line) and the carbon-fiber tract (lower white line). Comparison of *z*-scores ($n = 5$) shows a decrease in TH intensity 100 μm in diameter at the fused-silica tract (90 μm diameter) compared to control but not at the carbon-fiber tract. **(b)** Comparison of microsensor sensitivity to dopamine after one ($n = 5$), two ($n = 5$), or four ($n = 4$) months of implantation. The sensitivity of each

microsensor was assessed with flow injection analysis and was found to be unchanged over the time course assessed. Data are presented as mean ± s.e.m. **(c)** Voltammetric signal and corresponding background-subtracted cyclic voltammogram (inset) in response to stimulation of the ventral tegmental area (60 Hz, 24 pulses at 120 μA; left panel, red horizontal bar) or reward delivery (right panel, red triangle) in the same animal and on the same day. The pseudocolor plots depict color-coded observed changes in redox currents as a function of applied potential (y-axis) plotted over time (x-axis).

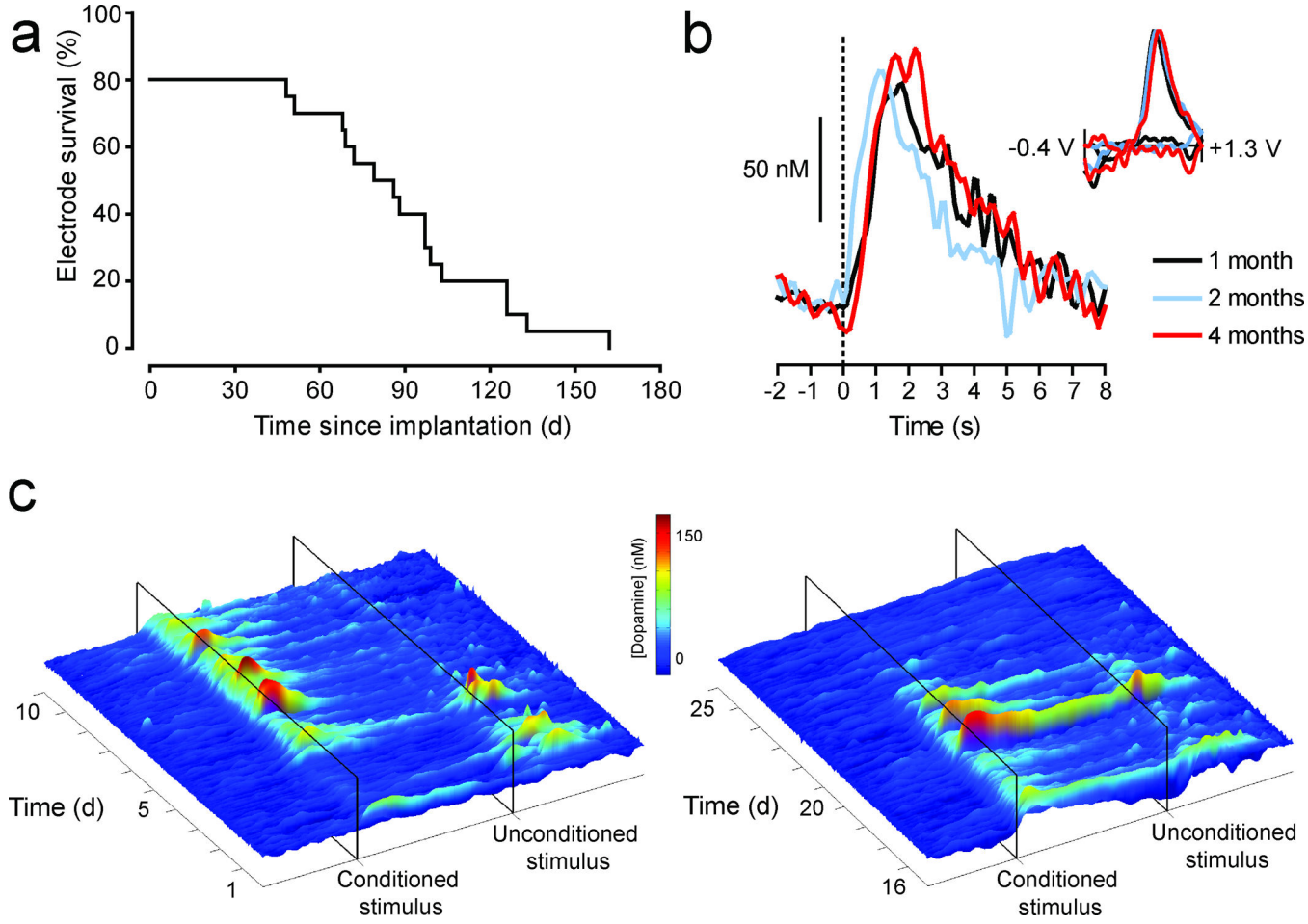

Figure 3. Long-term fidelity of chronic microsensors *in vivo*

(a) A survival curve depicting the attrition rate of chronic microsensors as a function of time since implantation. A microsensor was classified as "viable" if an electrochemical signal elicited by reward delivery met criterion for dopamine where it was statistically correlated with a background-subtracted cyclic voltammogram obtained from electrically evoked dopamine ($r^2 \geq 0.75$). **(b)** Voltammetric signals in response to reward delivery at time zero, one (black), two (blue) and four (red) months post-implantation. Background-subtracted cyclic voltammograms are all consistent with the electrochemical signature for dopamine (inset). **(c)** Voltammetric signals in response to reward delivery (unconditioned stimulus) and a predictive cue (conditioned stimulus) during pavlovian conditioning. The surface plots show trial-by-trial fluctuations in dopamine concentration during the twenty-second period around reward and cue presentation during acquisition (days 1–10, left plot), a period when the reward value was increased from one to four food pellets (days 16–20, right plot), and extinction (days 21–25, right plot) in a representative animal. The probability of approach to the cue increased during training (0.0 on day 1 to 1.0 on day 5), remained stable through day 10 (0.92), and decreased after extinction training (0.80 on day 20 to 0.12 on day 25) as did the cue-evoked dopamine response.